Step decoration of chiral metal surfaces

Jeong Woo Han,[1] John R. Kitchin,[2] and David S. Sholl[1,a)]
[1]*School of Chemical and Biomolecular Engineering, Georgia Institute of Technology, 311 Ferst Drive, Atlanta, Georgia 30332-0100, USA*
[2]*Department of Chemical Engineering, Carnegie Mellon University, Pittsburgh, Pennsylvania 15213, USA*

(Received 28 October 2008; accepted 9 February 2009; published online 26 March 2009)

Highly stepped metal surfaces can define intrinsically chiral structures and these chiral surfaces can potentially be used to separate chiral molecules. The decoration of steps on these surfaces with additional metal atoms is one potential avenue for improving the enantiospecificity of these surfaces. For a successful step decoration, the additional metal atoms should ideally remain at the kinked step sites on the surface. We performed density functional theory (DFT) calculations to identify pairs of metal adatoms and metal surfaces where this kind of step decoration could be thermodynamically stable. These calculations have identified multiple stable examples of step decoration. Using our DFT results, we developed a model to predict surface segregation on a wide range of stepped metal surfaces. With this model, we have estimated the stability of step decoration without further DFT calculations for surface segregation for all combinations of the 3*d*, 4*d*, and 5*d* metals. © *2009 American Institute of Physics*. [DOI: 10.1063/1.3096964]

I. INTRODUCTION

Chirality is a crucial property of most biomolecules such as proteins and DNA, which are the basis of life on earth. Each biomolecule in life tends to take exclusively one chiral form. As a consequence, two enantiomers of a chiral species often exhibit extremely different bioactivities. For example, *S*-penicillaminum gives good efficacy as an antiarthritic but *R*-penicillaminum is extremely toxic.[1] Enantiomerically pure chiral compounds must therefore be produced for human dosage. This has led to an enormous market in pharmaceutical industry. In 2005, worldwide sales of enantiopure drugs were more than $US 225 billion.[2]

Heterogeneous catalysis can potentially play a useful role in chiral processing of molecules. Two general approaches are used for preparing enantioselective heterogeneous catalysts, as discussed in several reviews in this area.[3,4] One approach is to create chirality by irreversibly adsorbing chiral molecules as chiral modifiers on achiral surfaces.[5] It is well known that a solid surface can gain enantioselectivity through this method. The second method is to use intrinsically chiral surfaces, which are crystal planes with a surface structure lacking mirror symmetry.[6–8] These surfaces can be created by cutting a single crystal along certain high Miller index directions. Multiple experiments and theoretical studies have shown that intrinsically chiral surfaces can provide enantiospecificity for chiral molecules.[7,8] In this paper, we have focused on intrinsically chiral surfaces.

It would be useful to control the catalytic reactivity or tune the chemistry of intrinsically chiral surfaces with the goal of enhancing the enantiospecificity of these surfaces. Two possible approaches that can be considered toward this goal are to change the surface orientation or to make surfaces decorated with impurities. In general, fabricating decorated surfaces is possibly the more flexible of these approaches. This idea is closely related to the general concept of using bimetallic rather than pure metals in heterogeneous catalysis, where the simultaneous presence of two metal species opens up a wide range of potentially useful catalytic phenomena. Unfortunately, little fundamental information is available to indicate how this idea could be pursued for highly stepped surfaces. In this paper, we consider the decoration of chiral stepped metal surfaces with an additional metal species. For this idea to affect enantiospecific adsorption on a chiral surface, it would be desirable for the impurities deposited on a surface to preferentially decorate the kinked step edges that make the surface chiral. This outcome is not necessarily guaranteed, however. In fact, there are at least three possibilities after step decoration: the impurities can prefer to remain in the kinked sites, they may prefer to be located in the surface terrace, or they may dissolve into the bulk. The surface segregation energy, which is the energy required for moving an impurity from the inside of a host metal to the surface,[9] plays a key role in determining which phenomenon is dominant. Therefore, if we know surface segregation energies, we can infer the tendency of the movement of an impurity after step decoration.

First-principles calculations of surface segregation energy have proven to be useful in screening potential surface/impurity combinations. An important set of calculations was performed by Ruban *et al.*,[9] who calculated 552 surface segregation energies of single transition metal impurities in transition-metal hosts. That work only examined flat surfaces, so it is not obvious without further work how these results are related to the concept of decorating undercoordinated sites on stepped surfaces.

We want to study the tendency of surface segregation of isolated metal impurities on chiral metal surfaces. The aim of our work was to establish a database describing surface seg-

a)Author to whom correspondence should be addressed. Electronic mail: david.sholl@chbe.gatech.edu.

regation on chiral surfaces focusing on which impurity atoms will segregate to the kinked step edges. We pursued this task by performing a large number of density functional theory (DFT) calculations to theoretically predict surface segregation for selected examples. We have subsequently used these calculation results to develop a correlation that makes predictions of surface segregation phenomena on flat and stepped surfaces for all combinations of $3d$, $4d$, and $5d$ metals. We limit our attention to the enthalpic contributions to surface segregation energies in these materials. The configurational entropy associated with the large number of possible sites for an impurity in a bulk material means that the free energy for surface segregation always favors dissolution of an impurity into the bulk relative to a prediction made using the enthalpic contributions alone. In general, the balance between this entropic effect and the enthalpic contributions to surface segregation control the net concentration difference between bulk and surface sites. We also limited our attention to the behavior of isolated impurity atoms, which means we cannot comment on the possibility of aggregation of impurities on surfaces. Both of these restrictions are consistent with the treatment of surface segregation energies by Ruban *et al.*[9]

II. THEORY

The surface segregation energy of an isolated impurity is defined as the energy needed to transfer an impurity atom from the bulk to the surface.[9–13] It can be calculated as the difference between the total energy derivatives of the surface and the bulk with respect to impurity concentration in the single impurity limit.[9,12–15] That is,

$$\varepsilon_{\mathrm{segr}} \equiv \left.\frac{\partial \varepsilon_{\mathrm{surf}}}{\partial c_{\mathrm{surf}}}\right|_{c\to 0} - \left.\frac{\partial \varepsilon_{\mathrm{bulk}}}{\partial c_{\mathrm{bulk}}}\right|_{c\to 0}, \tag{1}$$

where $\varepsilon_{\mathrm{surf/bulk}}$ is the total energy per atom of a surface/bulk system and $c_{\mathrm{surf/bulk}}$ is the impurity concentration of the surface/bulk system. In order to calculate this with DFT, each derivative term of Eq. (1) may be written as

$$\left.\frac{\partial \varepsilon_{\mathrm{surf/bulk}}}{\partial c_{\mathrm{surf/bulk}}}\right|_{c\to 0} \approx \frac{\left[\frac{1}{K}E\left(\frac{1}{K}\right) - \frac{1}{K}E(0)\right]}{\left(\frac{1}{K}\right)} = E\left(\frac{1}{K}\right) - E(0), \tag{2}$$

where $E(x/K)$ is a DFT total energy for a supercell containing K atoms including x impurity atoms. For large enough supercells, the dilute concentration limit is satisfied and Eq. (2) is accurate. Combining Eqs. (1) and (2),

$$\varepsilon_{\mathrm{segr}} \approx \left[E_{\mathrm{surf}}\left(\frac{1}{M}\right) - E_{\mathrm{surf}}(0)\right] - \left[E_{\mathrm{bulk}}\left(\frac{1}{N}\right) - E_{\mathrm{bulk}}(0)\right]. \tag{3}$$

Here, the surface (bulk) supercell contains M (N) atoms. Rearranging Eq. (3),

$$\varepsilon_{\mathrm{segr}} \approx \left[E_{\mathrm{surf}}\left(\frac{1}{M}\right) + E_{\mathrm{bulk}}(0)\right] - \left[E_{\mathrm{surf}}(0) + E_{\mathrm{bulk}}\left(\frac{1}{N}\right)\right]. \tag{4}$$

In Eq. (4), each pair of terms in square brackets corresponds to a set of DFT calculation with $M+N$ total atoms and one impurity. With this definition, a negative $\varepsilon_{\mathrm{segr}}$ indicates that the impurity remaining on the surface is preferred energetically to the impurity dissolving into the bulk.

As mentioned above, this approach only examines the enthalpic contributions to surface segregation energies. Generically, an impurity in the bulk of a material will always have a larger configurational entropy than an atom on a surface, so this entropy will reduce the tendency for surface segregation to occur when the free energy for this segregation is considered. Our treatment also neglects the contributions to the free energy of surface segregation energy due to vibrational degrees of freedom in the bulk material or the free surface.

We performed plane wave DFT calculations using the Vienna *ab initio* simulation package with the ultrasoft pseudopotentials available in this package.[16] These calculations used the generalized gradient approximation with the Perdew–Wang 91 (Ref. 17) functional and a plane wave expansion with a cutoff of 241.6 eV. During geometry optimization calculations, this cutoff energy was increased by 30%. Total energy calculations were conducted using the residual minimization method for electronic relaxation, accelerated using Methfessel–Paxton Fermi-level smearing with a width of 0.2 eV. Geometries were relaxed using the conjugate gradient algorithm until the forces on all the unconstrained atoms were less than 0.03 eV/Å. The unit cell and k-point mesh used for the surface calculation in each individual case are given below in details for each calculation. For all surfaces, the supercell consisted of layers that had a thickness equivalent to six layers of the (111) supercell and a vacuum spacing of 14 Å. We embedded each impurity in the top and bottom layers in order to cancel out any dipole effects. This approach introduces an additional factor of 2 into the first square bracket in Eq. (3). For all bulk calculations, a $3\times3\times3$ Monkhorst–Pack k-point mesh was used with a $4\times4\times4$ primitive supercell. For both surface and bulk calculations, the DFT-optimized lattice constants, which are listed below in details of each calculation, were used. In all surface calculations, the lattice constant in the plane of the surface was fixed at the DFT-optimized value of the pure metal. In bulk calculations that included impurities, the lattice constant of the material was fully relaxed.

III. RESULTS AND DISCUSSION

A. Direct DFT calculations of surface segregation energies

The method described in Sec. II for calculating Eq. (1) with DFT calculations is different from some previous approaches.[9–15,18,19] To compare our approach with previous calculations, we compared the selected results for flat surfaces with the results of Ruban *et al.*[9] Ruban *et al.*[9] performed DFT within the local density approximation in con-

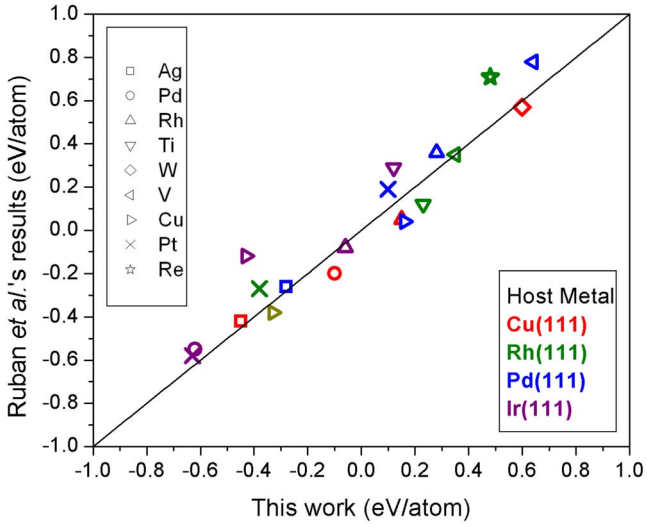

FIG. 1. (Color online) Comparison of our surface segregation energy results on Cu, Rh, Pd, and Ir(111) surfaces with Ruban *et al.* (Ref. 9).

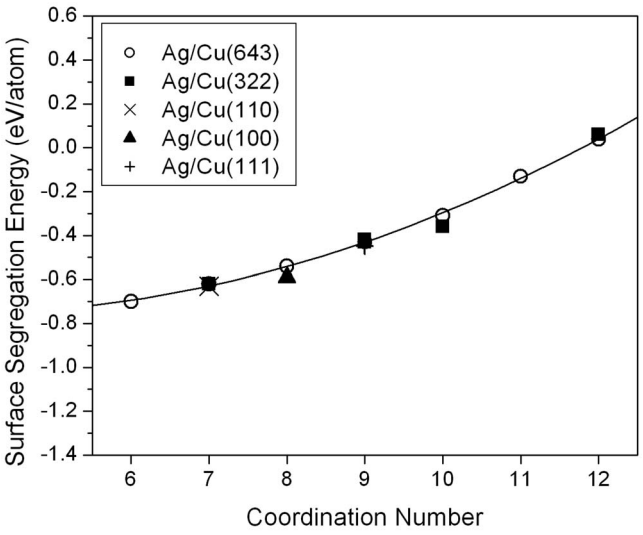

FIG. 2. Surface segregation energies of a Ag impurity on Cu surfaces.

junction with a Green's function technique to calculate the surface segregation energy of an isolated impurity on the most closely packed surface of the host metal. Their results are in good agreement with the available experimental data and previous DFT calculations.[20] We calculated the surface segregation energies of several impurities on Cu, Rh, Pd, and Ir(111) surfaces. In all, 19 impurity/surface combinations were included in this comparison, including examples with strong tendencies toward segregation, strong tendencies toward antisegregation, and examples with small segregation energies. A $4\times4\times1$ k-point mesh and a (3×3) surface unit cell were used for these surface calculations. The DFT-optimized lattice constants used for Cu, Rh, Pd, and Ir were 3.64, 3.85, 3.96, and 3.89 Å, in good agreement with the experimental values of 3.62, 3.80, 3.89, and 3.84 Å,[21] respectively. Figure 1 compares our results with the previous calculations of Ruban *et al.*; the root mean square deviation is 0.12 eV/atom.

The main aim of our calculations was to examine the segregation tendencies of impurity atoms on stepped surfaces. To do this, we examined a range of flat and stepped surfaces of fcc metals. Specifically, we examined the flat (110), (100), and (111) surfaces, which have 7, 8, and 9 coordinated sites, respectively, the stepped (322) surface, an achiral stepped surface with a (111) terrace and 7, 9, and 10 coordinated sites, and the chiral stepped (643) surface. The latter surface has sites with coordinations from 6–11. A $4\times4\times1$ k-point mesh was used for the (110), (100), and (111) surfaces with a (3×3) surface unit cell. A $2\times5\times1$ k-point mesh was used for the (322) surfaces with a (3×1) surface unit cell and a $3\times3\times1$ k-point mesh for the (643) surfaces with a (1×1) surface unit cell. Convergence tests indicated that these results were well converged in k-space.

For illustrative purposes, we first describe the surface segregation energies of a Ag impurity on Cu surfaces. Figure 2 shows the surface segregation energies for a Ag atom on various surface sites of the five Cu surfaces as a function of the coordination number (CN) of these sites. In Fig. 2, each symbol corresponds to each surface orientation and the black line is a quadratic fit to the data. The sites with CN=6 are the kinked step sites on Cu(643) and the sites with CN=12 are the subsurface sites. As mentioned in Sec. II, a negative surface segregation energy implies that segregation of an impurity toward the surface is enthalpically favored. The fact the segregation energy decreases and is negative as the CN is reduced indicates that on a stepped surface such as Cu(643), the sites with the lowest coordination will be preferentially decorated by Ag impurities compared to other sites on the surface.

We have performed calculations similar to those in Fig. 2 for four fcc host materials: Cu, Rh, Pd, and Ir. For each host, five impurities with various magnitudes of surface segregation energies for the (111) surface of the host as calculated by Ruban *et al.*[9] were chosen. Specifically, we examined Ag, Pd, Rh, Ti, and W impurities on Cu surfaces [Fig. 3(a)], Cu, Pt, Ti, V, and Re impurities on Rh surfaces [Fig. 3(b)], Ag, Cu, Pt, Rh, and V impurities on Pd surfaces

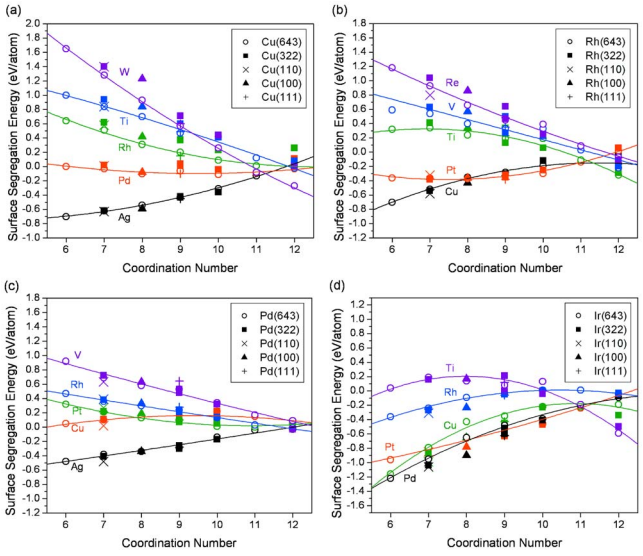

FIG. 3. (Color online) Surface segregation energies of 5 impurities on (a) Cu, (b) Rh, (c) Pd, and (d) Ir surfaces.

[Fig. 3(c)], and Pd, Pt, Cu, Rh, and Ti impurities on Ir surfaces [Fig. 3(d)]. In Fig. 3, each color corresponds to an impurity and each symbol to site on a specific surface. The curves associated with each data set are quadratic fits to the DFT data for each impurity/host combination. Clean Ir(110) is known to reconstruct, but our calculations examined the unreconstructed surface.

From these results, we can predict the possibility of step decoration for each binary pair. A negative value at CN=6 indicates that the segregation of an impurity would occur at the kinked step site. Therefore, it would be possible to decorate the kinked step site with Ag impurities on Cu surfaces, Cu and Pt impurities on Rh, Ag impurities on Pd, and Pd, Pt, Cu, and Rh impurities on Ir. On the other hand, due to positive values at CN=6, the following examples would be expected to dissolve into the bulk of each host after step decoration: Rh, Ti, and W impurities on Cu hosts; Ti, V, and Re impurities on Rh; Pt, Rh, and V impurities on Pd; and Ti impurities on Ir. It is also interesting to note that a Pd impurity on Cu surfaces does not show distinct CN dependency of its surface segregation and vice versa.

Our results at CN=12 are around zero but are not exactly zero. If surface segregation energies at CN=12 are measured in the bulk, they should be zero according to the definition of surface segregation in Eq. (1). However, we have calculated the surface segregation of CN=12 using subsurface sites that are right underneath the top surface layer. Even though these sites have CN=12, they may not be entirely in the bulk environment. Several reports have discussed the segregation of the impurities in subsurface layers.[10,12,15,19,22] These previous reports have also shown those segregation energies approach zero by approximately the 5th layer from the top surface.[10,15,22]

B. Development of a model for predicting surface segregation on stepped surfaces

Up to this point, we used DFT calculations of surface segregation energy to consider possible surface/impurity combinations for decorating surface steps. To consider the full range of binary transition metal pairs that exist, however, would require a huge number of DFT calculations. It is therefore worthwhile examining our DFT data to understand the physical trends that govern these results and to develop a model that can be applied to a larger group of surfaces.

1. Factors controlling segregation thermodynamics

In developing a model for surface segregation energies, it is critical to understand the physical origins of segregation. Here, we describe the contributions to these phenomena that have been observed in earlier work. Our observation that the surface segregation energy is strongly dependent on the CN is consistent with the previous reports.[23–26] This is physically plausible if segregation is described with a simple bond counting model.[23,24] The bond strength difference between the host and impurity is also an important factor in surface segregation.[23,26] There are multiple ways to characterize the bond strength of metals. High surface free energies are associated with high bond strengths and the surface free energy of a solid metal is ~1.2 times of that of liquid.[27] Thus, liquid surface tension can be used as a gauge of bond strength. The cohesive energy[28] or melting points of metals can also be used as a measure. These three approaches to describing bond strengths all show similar trends. This means that using one method is sufficient to investigate the correlation of bond strength with surface segregation. We used liquid surface tension data,[27] which are listed in Table S.1 of the supplementary information.[29]

The atomic size difference between host and impurity atoms has also been considered as another factor of surface segregation.[23,26,30] A large size mismatch between host and impurity atoms causes strain. It is typically expected that atoms of the component that has the larger radius segregate to the surface.[30] The nearest neighbor distance between atoms in the bulk[31] or the atomic radius[32] can be used as measures of atomic size. The Wigner–Seitz radius is a similar quantity.[33] All of these three definitions of atomic size are similar, so we used Wigner–Seitz radii[34] as the atomic size as listed in Table S.2 of the supplementary information.[29]

A final property that can play a role in surface segregation is the effects related to the metal *d*-bands.[9,24,25] Ruban *et al.* showed that surface segregation energy is related to the *d*-band width of metals.[9] In turn, Kitchin *et al.*[35] showed that the *d*-band width is related to the *d*-band center, which is defined as the centroid of the *d*-band density of states in an atomic sphere centered at a surface atom.[34] This implies that the *d*-band center should be correlated with surface segregation. When surface sites are doped with a second metal atom, the shift in the *d*-band center from the pure surface occurs. We used these shifts in *d*-band centers of surface impurities relative to the clean metal values to represent *d*-band properties. We performed simple DFT calculations to obtain *d*-band center values on the close packed surfaces of all the materials described below. For all calculations, the supercell consisted of six layers and a vacuum spacing of 14 Å as before. A (3×3) surface unit cell was used for fcc(111) and hcp(0001) surfaces and a (2×2) surface unit cell for bcc(110) surface. Spin-polarization effects were considered in the calculations for all impurities on Fe, Co, and Ni hosts and Fe, Co, and Ni impurities on all host materials. Crucially for the efficiency of this approach, no surface relaxation was included in these calculations. The results are listed in Table S.3 of the supplementary information.[29]

2. Correlations for predicting step decoration thermodynamics

A wide range of correlations between our DFT data in Sec. III A and the factors described in Sec. III B 1 were investigated. Among all the expressions we examined, the most effective correlation for a surface site with CN was

$$\varepsilon_{segr} = \Delta CN \times (0.158 \times \Delta\varepsilon + 0.062 \times \Delta d) - 0.060, \quad (5)$$

where ΔCN is $12-CN$, $\Delta\varepsilon$ is the bond strength difference, and Δd is the shift in *d*-band center between the impurity on the flat unrelaxed surface and the pure flat surface, respectively, with all energies in eV. The details of our calculations to determine the most effective correlation are in the supple-

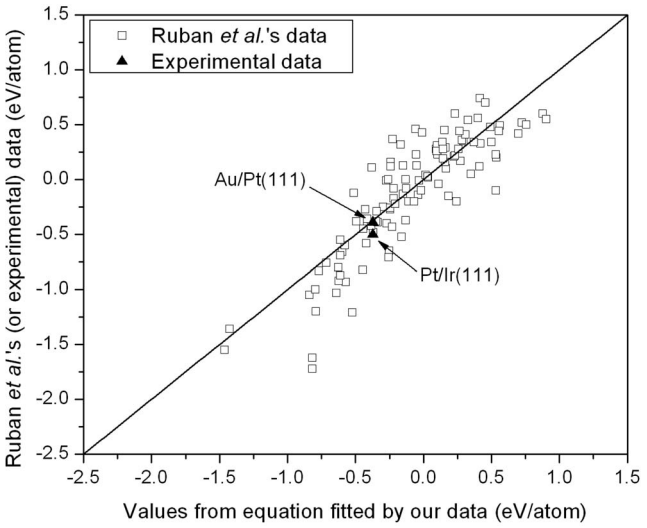

FIG. 4. Comparison of surface segregation energies of binary pairs of all fcc transition metals and Fe, Co, and Ru from our correlation with previous DFT and experimental data on the close packed surfaces. Open squares are for the data of Ruban *et al.* (Ref. 9) and filled triangles for experimental data (Ref. 37).

mentary information.[29] These calculations compared possible models with different numbers of model parameters using the leave one out method.[36] It is interesting to note that including the atomic size term discussed above does not significantly improve the description of the data. This may be explained by noting that the *d*-band center depends sensitively on atomic size,[34] so little additional information is gained by including atomic size in an expression that already incorporates a *d*-band center term. A number of the data sets for individual impurity/surface pairs show indications of a nonlinear dependence of the segregation energy on CN (see Figs. 2 and 3). Including a quadratic dependence of the segregation energy on CN did not, however, improve the description of the overall data set in a statistical way, so the expression above involves only a linear dependence on the CN.

An important feature of Eq. (5) is that it makes predictions about a range of surface sites. For example, using CN=9 for fcc and hcp, CN=6 for bcc into Eq. (5), we can predict the surface segregation energy on close packed surfaces of these hosts. The segregation energy associated with kinked stepped sites is predicted by Eq. (5) with CN=6 for fcc and hcp hosts and CN=4 for bcc hosts. This expression can also be used to describe the relative energies of pairs of surface sites with different CNs. For instance, based on Eq. (5), for an fcc material, the energy difference between an impurity on a (111) terrace site (CN=9) and a kinked step site (CN=6) is the same as that of an impurity from the bulk (CN=12) to the (111) terrace (CN=9). This means that the extensive data compiled by Ruban *et al.*[9] for the latter case can also be interpreted in terms of the distribution of impurity atoms among less coordinated surface sites.

In this paper, our focus has been concentrated on predicting the possibility of step decoration. Below, we use the correlation defined above to examine the surface segregation energies of a wide range of surface/impurity pairs on the kinked stepped surfaces.

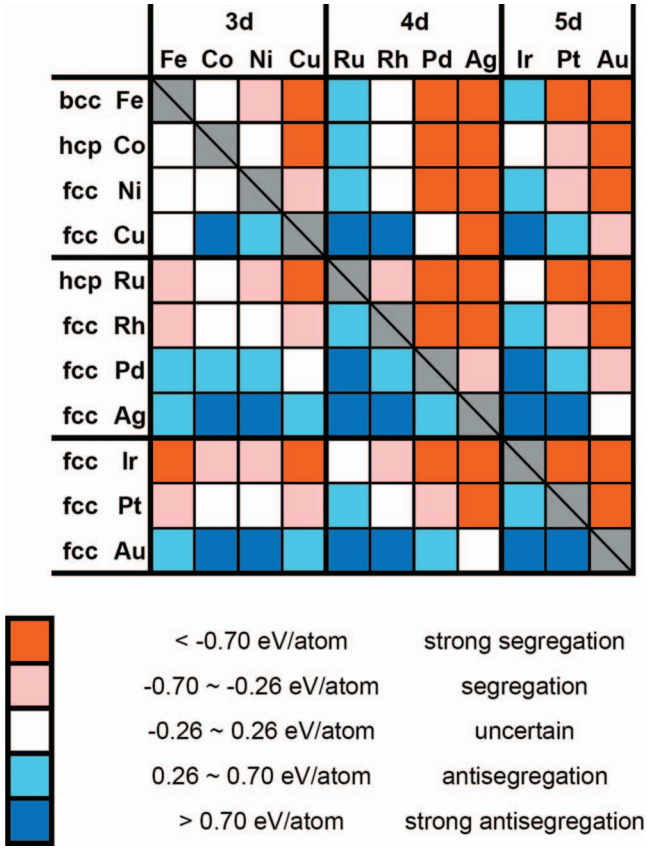

FIG. 5. (Color) Results for binary pairs of all fcc transition metals and Fe, Co, and Ru. These results were gained from Eq. (5) by substituting CN to 6. The sites with CN=6 correspond to kinked sites for fcc or hcp metals. Host metals (impurity metals) are listed vertically (horizontally).

C. Possible step decorations on the kinked step site

1. Application of the correlation to fcc, Fe, Co, and Ru hosts

In order to test the suitability of Eq. (5) for a broader data set, we compared the predictions of this correlation with the data of Ruban *et al.* for atomically flat surfaces.[9] This comparison was first performed with binary pairs of all fcc transition metals and Fe, Co, and Ru. Figure 4 shows this comparison. Two available surface core level shift (SCLS) experimental data points[37] that provide quantitatively reliable values of segregation energy[9] are also included in Fig. 4. In the Z+1 approximation, the SCLS can be interpreted as the segregation energy of an atomic number (Z+1) substitutional impurity in an atomic number Z host metal.[9,37] Overall, there is a good agreement between Eq. (5) and the data of Ruban *et al.* and good agreement with the experimental values is observed. The standard deviation between our correlation and the data of Ruban *et al.*[9] is 0.26 eV/atom. When considering the surface segregation properties of many impurity/host pairs semiquantitatively, the sign of the surface segregation energy is perhaps the most fundamental property of interest. Figure 4 suggests that when the absolute value of the surface segregation energy is larger than ~0.26 eV/atom, our correlation can reliably predict the sign of surface segregation energy.

Using Eq. (5), the possibility of decorating kink sites on

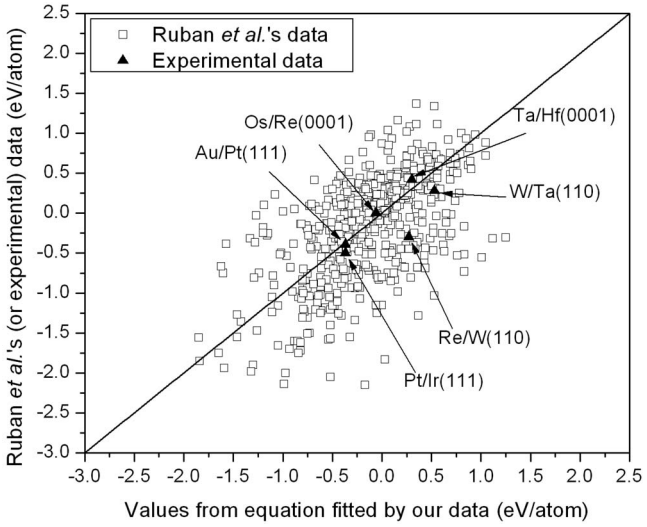

FIG. 6. Comparison of surface segregation energies of binary pairs of whole 3*d*, 4*d*, and 5*d* transition metals from our correlation with previous DFT and experimental data on the close packed surfaces. Open squares are for the data of Ruban *et al.* (Ref. 9) and filled triangles are for experimental data (Ref. 37).

chiral surfaces for a large number of examples can be assessed without further DFT calculations of surface segregation. Figure 5 shows the outcome of this analysis for 88 examples. In Fig. 5, each color corresponds to the magnitude of each bimetallic pair surface segregation energy for a kinked step site. Red colors indicate pairs with negative segregation energies, that is, examples where selective step edge decoration may be thermodynamically favored, while blue colors correspond to positive segregation energies. A number of entries in Fig. 5 are white. These are examples where we cannot reliably make a prediction using Eq. (5) because the absolute values of surface segregation energy from this expression are less than 0.26 eV/atom.

2. Application of the correlation to a larger class of metals

We also applied Eq. (5) to the full range of 3*d*, 4*d*, and 5*d* metals. Similar to Sec. III C 1, we compared the results on the close packed surfaces from our correlation with Ruban *et al.*[9] and six SCLS experimental measurements.[37] This comparison is shown in Fig. 6. A good agreement with the experimental values is observed, but the agreement with the data of Ruban *et al.*[9] is not quite as good as for the smaller data set examined in Fig. 5. The scattering mainly comes from surface segregation on bcc(110) surfaces. This presumably occurred because we only used DFT data from surface segregation on fcc hosts to construct our correlation. Nevertheless, when the absolute value of the surface segregation energy is larger than ~0.54 eV/atom, the standard deviation between our correlation's predictions and the data of Ruban *et al.*, we still reliably predict the sign of surface segregation for any combination of the 3*d*, 4*d*, and 5*d* metals.

The results of our DFT-based correlation are summarized in Fig. 7. The numbers used in Fig. 7 are also listed in Table S.8 of the supplementary information.[29] These results

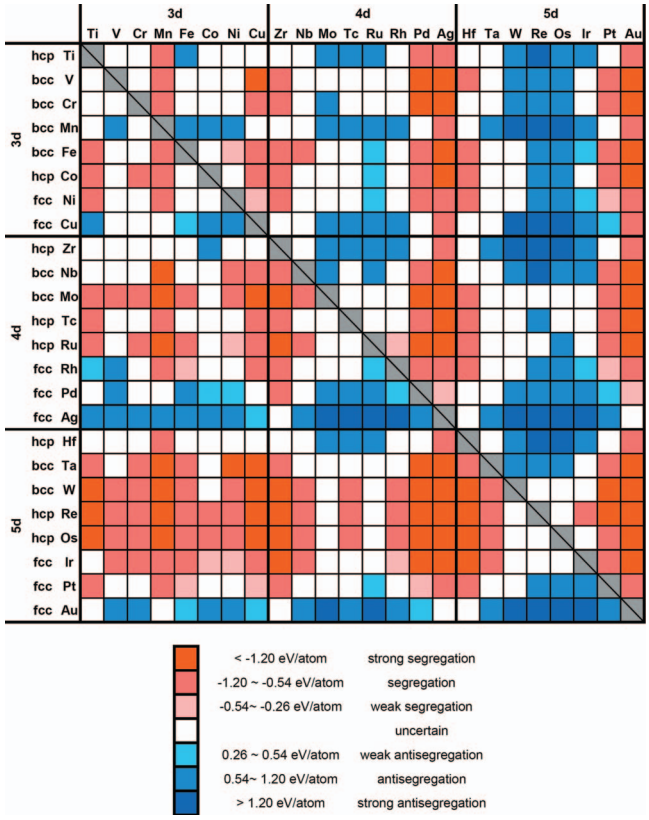

FIG. 7. (Color) Results for binary pairs of all 3*d*, 4*d*, and 5*d* transition metals. These results were gained from Eq. (5) by substituting CN to 6 (fcc or hcp) or 4 (bcc). The sites with CN=6 (4) correspond to kinked sites for fcc or hcp (bcc) metals. Host metals (impurity metals) are listed vertically (horizontally).

are obtained from Eq. (5) by setting CN to 6 (fcc or hcp) or 4 (bcc) to consider kinked sites on the surfaces. For the full range of 3*d*, 4*d*, and 5*d* metals, predictions in this figure are limited to cases where $|\varepsilon_{segr}|$ is larger than 0.54 eV/atom. For the materials shown in Fig. 5, the results for the range of $0.26 \leq |\varepsilon_{segr}| \leq 0.54$ eV/atom are included in Fig. 7. Figure 7 also includes predictions from the direct DFT results we described in Sec. III A. In all, a firm prediction can be made for 347 impurity/host pairs. Of these, 206 pairs are predicted to be situations where it may be thermodynamically favorable to selectively decorate undercoordinated step sites. For the remaining 141 pairs, this kind of step decoration is predicted to be thermodynamically unfavorable. Our results predict that step decoration is favored for many impurities on Mo, Ru, W, Re, Os, and Ir surfaces, while it would be unstable for almost all impurities on Ag and Au.

IV. CONCLUSION

We have examined step decoration thermodynamics using DFT calculations. Our calculations have identified many "step decorators" that are stable with respect to segregation into other surface sites or the bulk. Our work has used two approaches to contribute to the goal of controlling step decoration of chiral metal surfaces. First, we used detailed DFT calculations for dozens of examples to show that examples exist where decoration of kink sites on chiral surfaces is thermodynamically stable. Prior to these calculations, no evi-

dence was available to support or disprove this claim. Second, based on the DFT data, we developed a robust correlation suitable for characterizing surface segregation on stepped surfaces. This correlation was a useful tool for considering step decoration for hundreds of examples. Figure 7 showed the final results of this investigation.

When we predict or explain the results of step decoration only with Fig. 7, we should be appropriately cautious, noting that this treatment did not consider the kinetics of the deposition, diffusion, and growth that will be relevant in specific experiments. In addition, in examples where strong segregation of impurities is predicted, aggregation of impurities on the surface might occur. Even though our results neglected these effects, they still provide a useful basis for selecting surface/impurity pairs where these other aspects of step decoration could fruitfully be pursued.

Decoration of step edges on chiral metal surfaces may be an interesting avenue for tuning the surface chemistry of these materials. Chiral metal surfaces tuned by stable step decorations (such as the red colored bimetallic pairs in Fig. 7) may show enhanced enantiospecificity for chiral molecules binding on these surfaces. Further investigations would be necessary to find whether the adsorption of chiral molecules on step decorated chiral metal surfaces yields significantly different binding energies for two enantiomers of an adsorbing molecule or not. These results could then be compared to previous DFT calculations of small molecule adsorption on pure chiral surfaces.[4,8]

This kind of step decoration we have discussed here may also be applied to the development of tailored bimetallic nanoparticles for heterogeneous catalysis applications. Because nanoparticles usually have a large number of step edge and other undercoordinated surface sites, stable step decoration of a second metal on the surfaces would considerably affect their reactivity as catalysts. Our results may be useful for providing insight into materials where these kinds of effects can be contemplated.

ACKNOWLEDGMENTS

J.H. and D.S.S. acknowledge the support from the NSF through Grant No. 0717978 and useful conversations with Lymarie Semidey-Flecha.

[1] S. Lee, *Encyclopedia of Chemical Processing*, 2nd ed. (CRC, New York, 2005).
[2] S. Erb, Pharm. Technol. (October 3, 2006).
[3] D. S. Sholl, A. Asthagiri, and T. D. Power, J. Phys. Chem. B **105**, 4771 (2001); R. M. Hazen and D. S. Sholl, Nature Mater. **2**, 367 (2003); G. Held and M. Gladys, Top. Catal. **48**, 128 (2008).
[4] J. N. James and D. S. Sholl, Curr. Opin. Colloid Interface Sci. **13**, 60 (2008).
[5] L. A. M. M. Barbosa and P. Sautet, J. Catal. **217**, 23 (2003); S. M. Barlow and R. Raval, Surf. Sci. Rep. **50**, 201 (2003); B. Behzadi, A. Vargas, D. Ferri, K. H. Ernst, and A. Baiker, J. Phys. Chem. B **110**, 17082 (2006); K.-H. Ernst, Top. Curr. Chem. **265**, 209 (2006); A. Magistrato, A. Togni, and U. Rothlisberger, Organometallics **25**, 1151 (2006); A. Magistrato, T. K. Woo, A. Togni, and U. Rothlisberger, *ibid.* **23**, 3218 (2004); V. Nieminen, A. Taskinen, E. Toukonitty, M. Hotokka, and D. Y. Murzin, J. Catal. **237**, 131 (2006); A. Vargas, T. Burgi, and A. Baiker, *ibid.* **226**, 69 (2004); A. Vargas, F. Hoxha, N. Bonalumi, T. Mallat, and A. Baiker, *ibid.* **240**, 203 (2006); K. Tang, H. Gan, Y. Li, L. Chi, T. Sun, and H. Fuchs, J. Am. Chem. Soc. **130**, 11284 (2008); A. Baiker, J. Mol. Catal. A: Chem. **115**, 473 (1997); H. U. Blaser, H. P. Jalett, W. Lottenbach, and M. Studer, J. Am. Chem. Soc. **122**, 12675 (2000); M. Ortega Lorenzo, C. J. Baddeley, C. Muryn, and R. Raval, Nature (London) **404**, 376 (2000); S. M. Barlow and R. Raval, Curr. Opin. Colloid Interface Sci. **13**, 65 (2008); R. B. Rankin and D. S. Sholl, Surf. Sci. **548**, 301 (2004); R. B. Rankin and D. S. Sholl, *ibid.* **574**, L1 (2005); R. B. Rankin and D. S. Sholl, J. Phys. Chem. B **109**, 16764 (2005); R. B. Rankin and D. S. Sholl, J. Chem. Phys. **124**, 074703 (2006).
[6] C. F. McFadden, P. S. Cremer, and A. J. Gellman, Langmuir **12**, 2483 (1996); A. Kara and T. S. Rahman, J. Phys.: Condens. Matter **18**, 8883 (2006); A. E. Baber, A. J. Gellman, D. S. Sholl, and E. C. H. Sykes, J. Phys. Chem. C **112**, 11086 (2008).
[7] A. J. Gellman, J. D. Horvath, and M. T. Buelow, J. Mol. Catal. A: Chem. **167**, 3 (2001); J. D. Horvath and A. J. Gellman, J. Am. Chem. Soc. **123**, 7953 (2001); J. D. Horvath and A. J. Gellman, *ibid.* **124**, 2384 (2002); J. D. Horvath, A. Koritnik, P. Kamakoti, D. S. Sholl, and A. J. Gellman, *ibid.* **126**, 14988 (2004); D. M. Rampulla, A. J. Francis, K. S. Knight, and A. J. Gellman, J. Phys. Chem. B **110**, 10411 (2006); D. M. Rampulla and A. J. Gellman, Surf. Sci. **600**, 2823 (2006); A. Ahmadi, G. Attard, J. Feliu, and A. Rodes, Langmuir **15**, 2420 (1999); G. A. Attard, A. Ahmadi, J. Feliu, A. Rodes, E. Herrero, S. Blais, and G. Jerkiewicz, J. Phys. Chem. B **103**, 1381 (1999); G. A. Attard, *ibid.* **105**, 3158 (2001); R. Schillinger, Ž. Šljivancanin, B. Hammer, and T. Greber, Phys. Rev. Lett. **98**, 136102 (2007); A. Kuhnle, T. R. Linderoth, and F. Besenbacher, J. Am. Chem. Soc. **128**, 1076 (2006); D. S. Sholl, Langmuir **14**, 862 (1998); M. J. Gladys, A. V. Stevens, N. R. Scott, G. Jones, D. Batchelor, and G. Held, J. Phys. Chem. C **111**, 8331 (2007).
[8] Ž. Šljivancanin, K. V. Gothelf, and B. Hammer, J. Am. Chem. Soc. **124**, 14789 (2002); T. Greber, Ž. Šljivancanin, R. Schillinger, J. Wider, and B. Hammer, Phys. Rev. Lett. **96**, 056103 (2006); B. Bhatia and D. S. Sholl, Angew. Chem., Int. Ed. **44**, 7761 (2005); B. Bhatia and D. S. Sholl, J. Chem. Phys. **128**, 144709 (2008).
[9] A. V. Ruban and H. L. Skriver, Comput. Mater. Sci. **15**, 119 (1999); A. V. Ruban, H. L. Skriver, and J. K. Nørskov, Phys. Rev. B **59**, 15990 (1999).
[10] C. Jiang and B. Gleeson, Acta Mater. **55**, 1641 (2007).
[11] A. Saul and M. Weissmann, Phys. Rev. B **60**, 4982 (1999).
[12] M. Ropo, K. Kokko, L. Vitos, and J. Kollar, Phys. Rev. B **71**, 045411 (2005).
[13] M. Ropo, K. Kokko, L. Vitos, J. Kollar, and B. Johansson, Surf. Sci. **600**, 904 (2006).
[14] H. W. Hugosson, O. Eriksson, U. Jansson, and I. A. Abrikosov, Surf. Sci. **585**, 101 (2005).
[15] A. V. Ponomareva, N. V. Skorodumova, Y. K. Vekilov, and I. A. Abrikosov, Phys. Rev. B **75**, 245406 (2007).
[16] G. Kresse and J. Furthmüller, Comput. Mater. Sci. **6**, 15 (1996); G. Kresse and J. Hafner, Phys. Rev. B **48**, 13115 (1993).
[17] J. P. Perdew, J. A. Chevary, S. H. Vosko, K. A. Jackson, M. R. Pederson, D. J. Singh, and C. Fiolhais, Phys. Rev. B **46**, 6671 (1992).
[18] F. Qin, C. Jiang, J. W. Anderegg, C. J. Jenks, B. Gleeson, D. J. Sordelet, and P. A. Thiel, Surf. Sci. **601**, 376 (2007).
[19] O. M. Løvvik, Surf. Sci. **583**, 100 (2005).
[20] J. M. Howe, *Interfaces in Materials* (Wiley, New York, 1997); B. Nonas, K. Wildberger, R. Zeller, and P. H. Dederichs, Phys. Rev. Lett. **80**, 4574 (1998).
[21] ASM handbooks online, Materials Park, OH, 2002.
[22] A. V. Ruban, I. A. Abrikosov, D. Y. Kats, D. Gorelikov, K. W. Jacobsen, and H. L. Skriver, Phys. Rev. B **49**, 11383 (1994).
[23] F. F. Abraham, Phys. Rev. Lett. **46**, 546 (1981); F. F. Abraham and C. R. Brundle, J. Vac. Sci. Technol. **18**, 506 (1981); K. Wandelt and C. R. Brundle, Phys. Rev. Lett. **46**, 1529 (1981).
[24] S. Mukherjee, J. L. Moran-Lopez, V. Kumar, and K. H. Bennemann, Phys. Rev. B **25**, 730 (1982).
[25] P. Lambin and J. P. Gaspard, J. Phys. F: Met. Phys. **10**, 2413 (1980).
[26] D. Tomanek, A. A. Aligia, and C. A. Balseiro, Phys. Rev. B **32**, 5051 (1985).
[27] L. E. Murr, *Interfacial Phenomena in Metals and Alloys* (Addison-Wesley, Reading, MA, 1975).
[28] B. Farid and R. W. Godby, Phys. Rev. B **43**, 14248 (1991).
[29] See EPAPS Document No. E-JCPSA6-130-017912 for the procedures used to develop a correlation for predicting step decoration thermodynamics and the data used in Fig. 7. For more information on EPAPS, see http://www.aip.org/pubservs/epaps.html.

[30] H. Yamauchi, Phys. Rev. B **31**, 7688 (1985); A. Kiejna, J. Phys.: Condens. Matter **2**, 6331 (1990).
[31] M. J. Winter, WebElements: the first periodic table on the WWW, 2007.
[32] E. Clementi, D. L. Raimondi, and W. P. Reinhardt, J. Chem. Phys. **47**, 1300 (1967).
[33] A. P. Sutton, *Electronic Structure of Materials* (Oxford University Press, New York, 1993).
[34] A. Ruban, B. Hammer, P. Stoltze, H. L. Skriver, and J. K. Nørskov, J. Mol. Catal. A: Chem. **115**, 421 (1997).
[35] J. R. Kitchin, J. K. Nørskov, M. A. Barteau, and J. G. Chen, J. Chem. Phys. **120**, 10240 (2004).
[36] R. Drautz and A. Diaz-Ortiz, Phys. Rev. B **73**, 224207 (2006); H. A. Martens and P. Dardenne, Chemom. Intell. Lab. Syst. **44**, 99 (1998); L. Semidey-Flecha and D. S. Sholl, J. Chem. Phys. **128**, 144701 (2008).
[37] A. Flodstrom, R. Nyholm, and B. Johansson, *Advances in Surface and Interface Science* (Plenum, New York, 1992), Vol. 1.